NUMERICAL MODELLING OF WARM PRESTRESS EFFECT USING A DAMAGE FUNCTION FOR CLEAVAGE FRACTURE

F.M. Beremin[1]

Centre des Matériaux de
L'Ecole Nationale Supérieure des Mines de Paris
B.P. 87 - 91003 Evry Cédex, France

ABSTRACT

In order to simulate numerically the warm prestress effect on a A508 steel, several experiments have been performed on bulk and cracked specimens. The experiments on circumferentially notched tensile specimens show a variation in the critical stress for cleavage as a function of the amount of material involved in the fracture process. The tests on CT50 specimens and axisymmetrically cracked bars emphasize the role of residual stresses and the importance of crack blunting. A numerical simulation of the different experiments shows the different phenomena leading to the apparent strengthening of the material resulting from warm prestress effect.

KEYWORDS

Fracture; cleavage; warm prestress; A508; crack blunting; residual stresses; numerical calculations.

INTRODUCTION

The warmprestress effect is the apparent increase in toughness of a cracked body resulting from a previous loading applied at higher temperature. During the cooling of a cracked component, the stress intensity factor may happen to exceed the critical toughness K_{IC} without rupture(e.g. Bewitt and coworkers, 1964). Recent studies have clearly shown the importance of this phenomenon (Loss and coworkers, 1978, 1979). Different interpretations have been proposed (Chell, 1979; Curry, 1979). In particular, Curry (1979) adopted an approach very similar to the method used in this study.

---

[1]F.M. Beremin is a research group including Y. d'Escatha*, J.C. Devaux**, P. Ledermann*, F. Mudry*** and A. Pineau***, from :
* Bureau de contrôle de la construction nucléaire, 3, rue de Vosges, 21000 Dijon.
** Division des Fabrications de Framatome, B.P.13, 71380 Saint-Marcel.
*** Centre des Matériaux de l'Ecole des Mines de Paris, B.P. 87, 91003 Evry Cédex ERA CNRS n°767.

From this point of view, the reason for the apparent strengthening of the material must be sought in the conditions for cleavage fracture at the tip of a crack. A model for cleavage fracture has already been proposed by Ritchie, Knott and Rice (1973) on a steel containing a high content of nitrogen. This approach predicts the shape of the K_{IC} transition curve on the assumption that cleavage takes place when a critical normal stress σ_c is reached over a characteristic distance λ . The same approach has been used by Parks (1976) in the case of A533 steel.

The aim of this study is a prediction of the warm prestress effect on a A508 steel using a local cleavage criterion. A very important preloading at 100°C has been chosen in order to better analyse the phenomenon. This more severe loading sequence is the main difference with other studies. The first part is devoted to the determination of a criterion for cleavage fracture at -196°C whilst the second part analyses the effect of previous loading at higher temperature on the toughness at -196°C. Finally, a numerical calculation has been performed.

EXPERIMENTAL PROCEDURES AND RESULTS

Experiments on cleavage fracture at -196°C

The material under study is a A508 steel named steel A. It is taken from a nozzle shell of a PWR vessel. Its chemical composition and its mechanical properties at 100°C are presented in Table 1. Different specimen geometries have been used. Six of them are shown in Fig. 1 as well as their denomination used in this study. Most of these geometries have been analysed using the finite element method. The specimens named AE10, AE4 and AE2 have been computed with the stress-strain curve of steel A at 100°C. This calculation was made in another study (Beremin, 1980). The strain distribution at -196°C is assumed to be the same for the same value of the current minimum diameter $\emptyset$, whilst the stress distribution is supposed to be that at 100°C multiplied by the ratio of the yield stresses $\sigma_y(-196°C)/\sigma_y(100°C)$. Conventionnal tensile test as well as the AE20 specimens are interpreted using the Bridgman approximation (1964). The specimens AE0.2, $\theta = 45°$ and AE0.2, $\theta = 90°$ have been calculated by the finite element method using the stress - strain relationship of our steel at -196°C. At last, CT25 specimens were used to determine a valid K_{IC}.

TABLE 1

Steel	Chemical composition (Wt %)								Mechanical properties at 100°C		
	C	S	P	Si	Mn	Ni	Cr	Mo	$R_{0.2\%}$ (MPa)	R_T (MPa)	Σ(%)
A	0.144	0.009	0.011	0.185	1.225	0.70	0.26	0.510	421	553	72
B	0.152	0.010	0.006	0.3	1.25	0.84	0.20	0.49	395	540	73

All the specimens are broken at -196°C. The load P is continuously recorded. Except for the two AE0.2 specimens, the current diameter of the minimum section of the axisymmetric specimens is also recorded. All the experimental results are given in Table 2 where $\sigma = 4P/\pi\phi^2$ and $\varepsilon = 2\mathrm{Ln}\,\phi_o/\phi$, ϕ_o being the initial minimum diameter (ϕ_o = 10 mm). The maximum tensile stress in the minimum section σ_{Max} was assessed using the results of the mechanical analysis previously described.

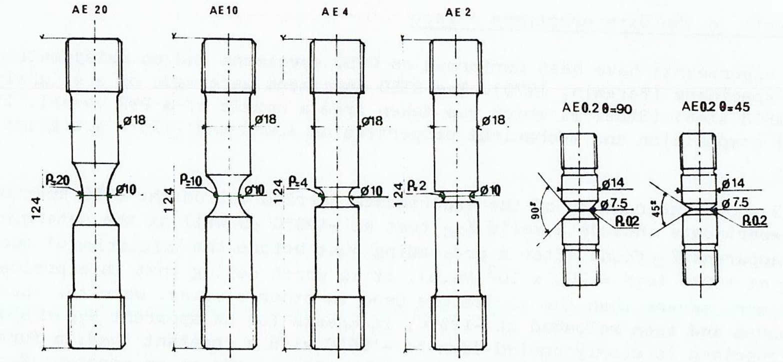

Fig. 1. Geometry of the specimens used.

TABLE 2 Experimental results on cleavage fracture at -196°C.

Less sharply notched specimens		Tensile specimens	AE 20	AE 10	AE 4	AE 2
Average stress at rupture	σ(MPa)	1424 1485	1163 1128 1187	1172 1164	1287 1314	1235 1170
Average strain at rupture	ε(%)	52 69	7.4 5.3 8.9	2.1 2.7	0.7 1.4	0.27 0.35
Maximum stress at rupture	σ_{max}(MPa)	1483 1571	1316 1288 1336	1421 1397	1420 1520	1460 1470
Sharply notched specimens		AE 0.2 θ = 45°		AE 0.2 θ = 90°		
Rupture load	$P(10^4 N)$	4.3 ± 1.3(10 specimens)		5 ± 1 (12 specimens)		
Maximum stress at rupture	σ_{max} (MPa)	1700 ± 100		1765 ± 10		
K_{IC} (MPa $\sqrt{m}$)		23.8 - 23.9 - 27.5 - 23.0 - 24.2				

It was observed that all specimens broke in a brittle manner along the minimum section. Scanning electron microscope observations clearly show that the fracture surfaces were typical of cleavage fracture. A metallographic analysis of a vertical section of some ruptured specimens showed a great number of secondary cracks. Near the center of the less sharply notched specimens, stable microcracks were seen. Thus, the fracture mechanism seems very similar to that of the steel investigated by Ritchie, Knott and Rice (1973). The initiation point of the fracture was difficult to find out. However, from visual inspection, it appeared that fracture originated near the center of the specimen for the notch radii greater than 3 mm and near the surface for the sharper notches. This is in agreement with the location of the maximum tensile stress in the minimum section, as already emphasized (Beremin, 1980).

Experiments on the warm prestress effect

Several experiments have been performed on CT50 specimens and on axisymmetrically cracked specimens (Beremin, 1979). The CT50 specimens were made of a slightly different A508 steel (Steel B) which was taken from a nozzle of a PWR vessel. Its chemical composition and mechanical properties at 100°C and -196°C are given in Table 1.

Figure 2 shows the results of the experiments carried out on the CT50 specimens. These experiments include a valid K_{IC} test at -196°C as well as the determination of the apparent K_{IC} found after a preloading just before the initiation of ductile tearing at 100°C (J_{IC} = 200 x 10^3 Pa.m). It is worth noting that this preloading is much more severe than the conditions used in other studies. When the specimen is unloaded and then reloaded at -196°C, it breaks for an apparent K_{IC} of 65 MPa$\sqrt{m}$. If the specimen is slowly cooled down to -196°C with a constant load, a further loading is necessary at this last temperature. This leads to an apparent K_{IC} of 118 MPa $\sqrt{m}$.

Figure 3 shows the results of the experiments carried out on axisymmetrically cracked specimens. The technique used for this kind of specimens is described by Hourlier and Pineau (1979). This specimen was chosen because it allows a simple 2D representation in a finite element program without any assumption about plane strain or plane stress state. The fracture toughness of steel A is 25 MPa $\sqrt{m}$. The loading sequences described in figure 3 show that an important warmprestress effect is also present for these specimens. The same trends as those observed in the CT specimens are noted e.g. cooling under constant load control results in an apparent toughness of 75 MPa $\sqrt{m}$ which is three times the measured valid K_{IC}.

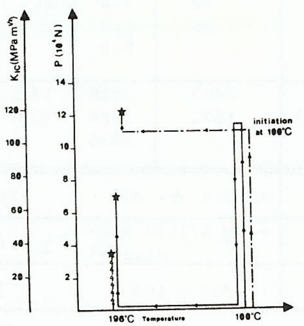

Fig. 2. Experimental results on CT50 specimens.

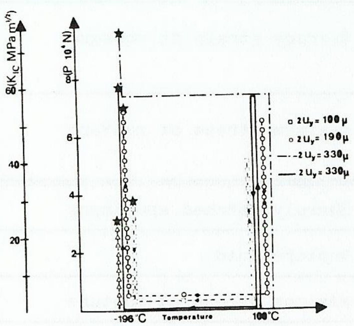

Fig. 3. Experimental results on axisymmetrically cracked specimens.

DISCUSSION

Cleavage fracture

If the results on AE0.2 specimens are not taken into account, it is clear that all the results can be explained by a fracture stress of 1430 MPa ± 90 MPa. However, this value is not readily applicable to the AE0.2 specimens where a more important scatter in the experimental results is noticed. It is felt that most results can be explained if we use a statistical analysis of fracture such as Weibull's theory (1939). In this case, bigger specimens or less sharply notched specimens will yield to lower values for σ_c. This trend is noticed in the experimental results if the tensile tests are disregarded because of their very high plastic strain at rupture. A more accurate calculation of this statistical effect can be realized. The critical fracture stress is a statistical, size dependent parameter. It is of order 1450 MPa when millimetric lengths are involved and around 1770 MPa with lengths of order 200 µm. Since the determination of the critical stress is usually done on sharply notched three points bend specimens, this latter value will be retained. Using the procedure proposed by Ritchie, Knott and Rice (1973), a characteristic distance λ of 45 µm is found with σ_c = 1770 MPa and K_{IC} = 24 MPa $\sqrt{m}$. This distance is about twice the grain size of our material which is consistent with the microscopic fracture model proposed by Ritchie, Knott and Rice (1973). These two value of σ_c and λ, which are equally close to those found by Parks (1976) and Curry (1979), are used in the following discussion.

Warm prestress effect

This effect can arise from three different reasons. First of all, the stress distribution at a crack tip after a prestressing at 100°C, is very different, for the same load, from that corresponding to a virgin material. The residual stresses must be subtracted. As a second reason, the crack tip has been blunted at 100°C and a finite radius exists at -196°C. Finally, the plastic deformation at higher temperature may have an effect on the cleavage process itself.

Some additional experiments have been performed to clarify these points. An axisymmetrically cracked specimen has been loaded just before crack initiation, then unloaded, stress relieved at 600°C under vacuum during two hours. A K_{IC} test at -196°C gives an apparent K_{IC} of 46 MPa $\sqrt{m}$ instead of 60 ± 5 MPa $\sqrt{m}$. Even if the annealing treatment was not sufficient, this experiment points out the effect of residual stresses. Some specimens have been loaded after crack initiation at 100°C, therefore destroying the crack blunting effect. When ruptured at -196°C, an apparent K_{IC} between 40 and 50 MPa$\sqrt{m}$ results. It is felt that the residual stresses account for around 20 MPa $\sqrt{m}$ in the warmprestress effect and crack blunting is responsible for about 15 MPa $\sqrt{m}$. A plastic deformation at 100°C may have an effect on the cleavage stress at liquid nitrogen temperature. Some tensile specimens which were given different overall deformation have been tested at -196°C. These further tests led to a slightly higher stress for cleavage fracture (Table 3). It should be noticed that this increase in σ_c is rather small as compared to the very high cumulated plastic strains applied in these experiments (up to 117%). These very high plastic deformations cannot take place in front of a crack tip except for very important C.O.D. applied at 100°C.

TABLE 3

Plastic strain during loading at 100°C	Maximum stresses and average stresses and strain at rupture at -196°C			Apparent yield point at -196°C
ε_{def} (%)	σ (MPa)	ε (%)	σ_{max} (MPa)	σ_y (MPa)
7.5 8	1567 1526	67 50	1650 1605	1020 1020
30 30	1702 1583 1683	54 46 56	1828 1690 1810	1187 1170 1181
100	1787	17	1970	1505

NUMERICAL SIMULATION

The axisymmetrically cracked specimens have been modelized with the finite element method. Since crack blunting appears to be an important parameter, two different meshes have been used; one with the ordinary technique without crack blunting modelisation, the second one involved a very small radius of curvature at the crack tip (10 µm). In this second case, a very small mesh size was necessary near the crack tip because of the very steep gradients of stresses and strains. It has been shown previously that this technique can account for crack blunting (d'Escatha and coworkers, 1979). Figure 4 shows the refined mesh as well as the loading conditions. An homogeneous displacement Uy is imposed on top of the specimen. The stress-strain constitutive equations used were those experimentally determined at 100°C and -196°C for strains lower than 10%. Above this value, linear strain hardening was assumed. (Beremin, this issue).

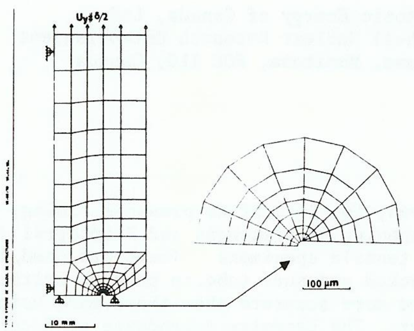

Fig. 4. Refined mesh near the crack tip.

Three different calculations have been performed. The refined mesh has been unloaded from displacement 2Uy = 100 µm and 2Uy = 190 µm. When the load was zero, the characteristics of the material (Young's modulus, yield stress) were changed from those at 100°C to those at -196°C. Uy was then increased again up to the experimentally observed toughness (between 53 and 58 MPa $\sqrt{m}$ for 2Uy = 190 µm and between 30 and 32 MPa $\sqrt{m}$ for 2Uy = 100 µm). Another calculation was made with the other mesh without crack blunting modelisation. When 2Uy = 330 µm (initiation point at 100°C), the material characteristics are changed under constant load conditions. Then the displacement was again increased up to the experimentally observed fracture (between 73 MPa $\sqrt{m}$ and 76 MPa $\sqrt{m}$). This mesh without blunting contains bigger element sizes in front of the crack tip (≃ 200 µm). The difference between the two meshes is not significant at distances larger than 400 µm from the crack-tip. This permits the use of the less refined mesh for this last calculation.

NUMERICAL RESULTS AND DISCUSSION

Figure 5 shows the calculated stress distributions in front of the crack tip. A distribution for a K_{IC} of 26 MPa $\sqrt{m}$ corresponding to the virgin material has also been computed. This last distribution is very close to that used by Ritchie, Knott and Rice (1973). It is seen that a critical stress of 1770 MPa over a distance λ = 45 µm can reasonnably explain the virgin K_{IC} as well as the specimen warmprestressed with 2Uy = 100 µm. However, the examination of the stress distribution corresponding to 2Uy = 190 µm shows that the same value for σ_c leads to a much higher value for λ. In the latter case the plastic zone at 100°C is very large and the equivalent plastic strain cumulated near the crack tip is important (around 15% at 100 µm from the crack tip and 80% in the nearest element). This probably increases the cleavage resistance of the material. From experiments on tensile tests, a strain of 30% yields to a 19% higher fracture stress. Therefore, a critical stress around 2100 MPa must be used in this case over the same distance of 50 µm. Figure 4 shows that these values are consistent with the stress distribution corresponding to 2Uy = 190 µm.

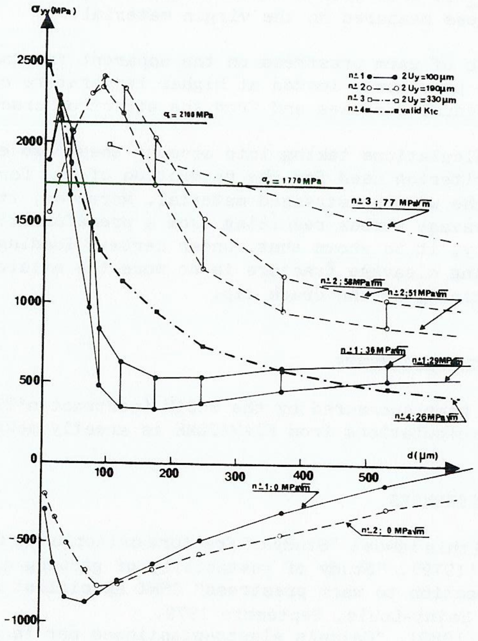

Fig. 5. Calculated stress distributions in front of the crack tip.

For the last experiment, in the load controlled case, another phenomenon appears. When the characteristics of the material are changed, the structure becomes entirely elastic until the apparent K_{IC} reaches 73 MPa $\sqrt{m}$. For 77 MPa $\sqrt{m}$, only three integration points of the first 8 nodes element are plastic. Therefore, in this case, the critical event must be the beginning of plastic deformation which immediately initiates unstable microcracks. However the plastic strain at 100°C must be elevated and can induce also an important strengthening. From this discussion, it appears that for weak prestressing, the interpretation of the warmprestress effect is relatively clear. It arises mainly from residual stresses and from the effect of crack blunting. For more severe prestressing, more complicated phenomena must be included such as strengthening induced by plastic strain. The last experiment clearly shows another aspect of the warmprestress effect. Under these conditions a considerable value for K has to be applied before plastification begins. In these conditions the attainment of plastic deformation over a characteristic distance in front of the crack tip is the critical step for cleavage fracture.

CONCLUSIONS

1. The cleavage fracture stress measured on circumferentially notched tensile specimens is a function of the amount of material involved in the process of brittle fracture.

2. The application of a criterion which involves a critical stress (σ_c = 1770 MPa $\pm$ 60 MPa) over a characteristic distance ($\lambda \simeq 50$ µm) can account for fracture toughness measured on the virgin material.

3. The influence of warm prestress on the apparent fracture toughness of specimens which have been previously loaded at higher temperature can be inferred from the analysis of residual stresses and from the effect of crack blunting.

4. Numerical calculations taking into account these two effects indicate that the same type of criterion used for the prediction of K_{IC} for the virgin material can be applied to the warm prestressed material. Moreover, it is shown that the increase in cleavage stress resulting from a predeformation has to be taken into account. Finally, it is shown that, under certain loading conditions, the critical event controlling cleavage fracture is no more the attainment of σ_c over λ but the advent of plasticity at the crack tip.

ACKNOWLEDGMENTS

This study has been sponsored by the SCSIN (contract n°296.686). Financial support for numerical computations from FRAMATOME is greatly acknowledged.

REFERENCES

Beremin, F.M. (this issue). "Study of fracture criteria for ductile rupture of A508 steel".
Beremin, F.M. (1979). "Study of instability of growing cracks using damage functions. Application to warm prestress" CSNI specialist meeting on plastic tearing instability. Saint-Louis, Septembre 1979.
Beremin, F.M. (1980). "Calculs elasto-plastiques par la méthode des éléments finis d'éprouvettes axisymétriques entaillées circulairement" to appear in Journal de mécanique appliquée.
Bewitt, E., A. Cowen and S. Stott (1964). J. Brit. Nucl. Eng. Soc., January, 1-17
Bridgman, P.W. (1964) in "Studies in large plastic flow and fracture" Harvard University press, Cambridge, Massachussets.
Chell, G.C., J.R. Haigh and V. Vitek (1979). CERL Report n° RD/L/N63/79.
Curry, D.A. (1979). CERL Report n° RD/L/N103/79.
d'Escatha, Y., J.C. Devaux, P. Ledermann and F. Mudry (1979). 5th SMIRT Conf. Berlin August 1979.
Hourlier, F., and A. Pineau (1979). Mémoires scientifiques de la revue de métallurgie, March 1979, 175-179.
Loss, F.J., R.A. Jr. Gray and J.R. Hawthorne (1978). J. Nucl. Engn. Design., 46. 395-408.
Loss, F.J., R.A. Jr. Gray and J.R. Hawthorne (1979). Trans. ASME. J. Press. Techn., 298-304.
Parks, D.M. (1976). Trans. ASME, J. Eng. Mat. Techn. January, 30-35.
Ritchie, R.D., J.F. Knott and J.R. Rice (1973). J. Mech. Phys. Solids, 21, 395-410.
Weibull, W., (1939). Ing. Vetenskaps Akad. Handl., 153.